iScience

CellPress

Article

# Over 14% Efficiency Folding-Flexible ITO-free Organic Solar Cells Enabled by Eco-friendly Acid-Processed Electrodes

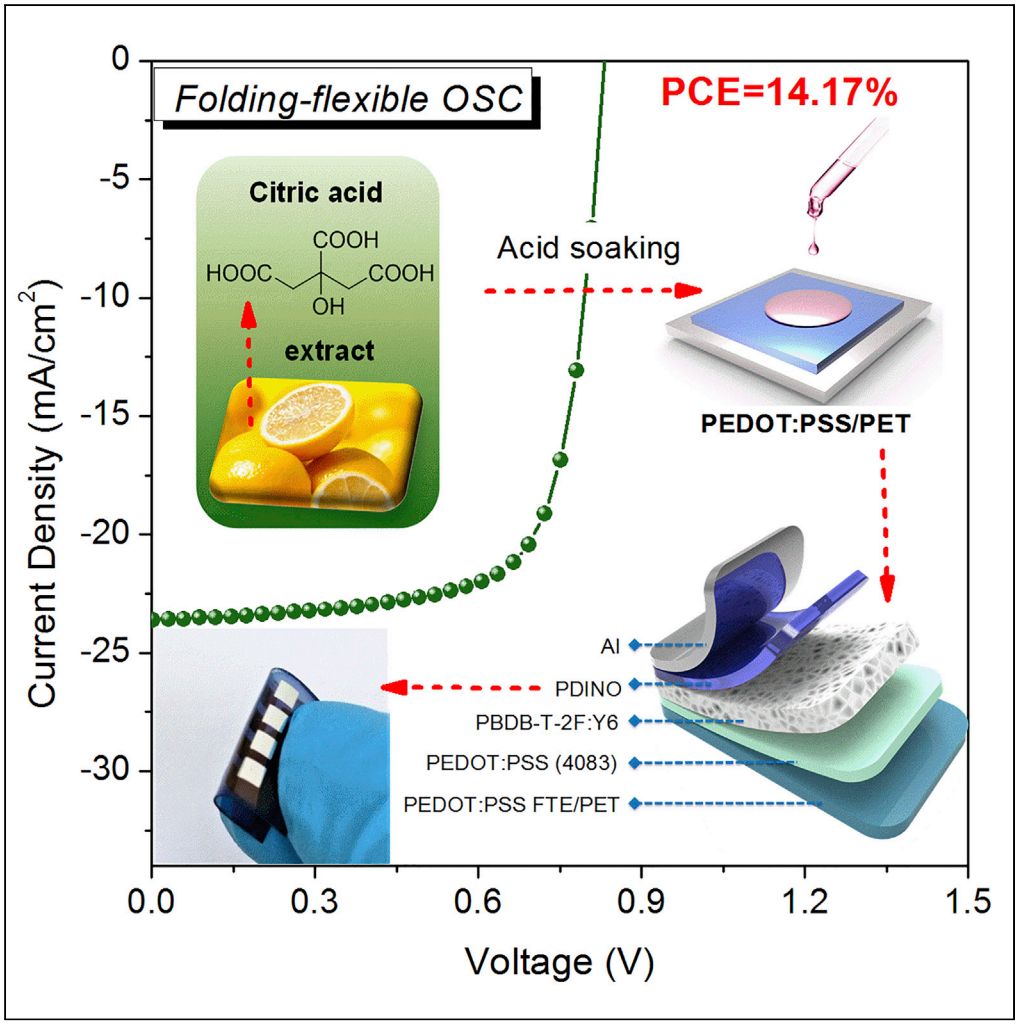


Wei Song, Ruixiang Peng, Like Huang, ..., Jinfeng Ge, Antonio Facchetti, Ziyi Ge

geziyi@nimte.ac.cn

## HIGHLIGHTS

Highly conductive PEDOT:PSS electrodes based on eco-friendly acid were exploited

14.17% folding-flexible organic solar cells were realized

The bending performance was significantly improved by interface bonding engineering

Song et al., iScience *23*, 100981
April 24, 2020 
https://doi.org/10.1016/j.isci.2020.100981

iScience

CellPress

Article

# Over 14% Efficiency Folding-Flexible ITO-free Organic Solar Cells Enabled by Eco-friendly Acid-Processed Electrodes

Wei Song,[1,2] Ruixiang Peng,[1,2] Like Huang,[1] Chang Liu,[1] Billy Fanady,[1] Tao Lei,[1,2] Ling Hong,[1,2] Jinfeng Ge,[1] Antonio Facchetti,[3] and Ziyi Ge[1,2,4,*]

## SUMMARY

**Environment-friendly manufacturing and mechanical robustness are imperative for commercialization of flexible OSCs as green-energy source, especially in portable and wearable self-powered flexible electronics. Although, the commonly adopted PEDOT:PSS electrodes that are treated with severely corrosive and harmful acid lack foldability. Herein, efficient folding-flexible OSCs with highly conductive and foldable PEDOT:PSS electrodes processed with eco-friendly cost-effective acid and polyhydroxy compound are demonstrated. The acid treatment endows PEDOT:PSS electrodes with high conductivity. Meanwhile, polyhydroxy compound doping contributes to excellent bending flexibility and foldability due to the better film adhesion between PEDOT:PSS and PET substrate. Accordingly, folding-flexible OSCs with high efficiency of 14.17% were achieved. After 1,000 bending or folding cycles, the device retained over 90% or 80% of its initial efficiency, respectively. These results represent one of the best performances for ITO-free flexible OSC reported so far and demonstrate a novel approach toward commercialized efficient and foldable green-processed OSCs.**

## INTRODUCTION

Flexible optoelectronic and microelectronic devices have attracted significant attentions due to their merits in terms of flexibility, lightweight, low cost production, and future prospects for roll-to-roll production (Kim et al., 2013; Min et al., 2014; Zhao et al., 2017), which are all crucial for wearable and mobile devices (Ling et al., 2018; Jinno et al., 2017; Park et al., 2018; Søndergaard et al., 2012; Wen et al., 2018; Worfolk et al., 2015). In these applications, mechanically durable power sources are very important component. Flexible organic solar cells (Fl-OSCs), in particular, are currently attracting much interest as a promising clean-energy technology (Yan et al., 2018; Qian et al., 2018; Baran et al., 2017). With their flexibility, Fl-OSCs play a crucial role as a continuous source of energy supply in those wearable and mobile devices (Song et al., 2018; Peng et al., 2019; Zhang et al., 2019; Sun et al., 2015). However, for some extreme applications, such as thin-film electronics on textiles (clothes and self-powered bags) and other three-dimensional curved surfaces (folding airships), flexibility alone is not enough, as foldability is also urgently required. This quickly promoted the concept and research of foldable organic solar cells (Fo-OSC) (Cheng et al., 2016b, 2016a; Zhou et al., 2018). Although, conventional organic solar cells (OSCs) commonly utilized indium tin oxide (ITO) as the transparent electrode material, which suffers from its high cost and mechanical brittleness (Xia et al., 2012; Yeon et al., 2015; Worfolk et al., 2015; Song et al., 2019). These factors have limited the applications of ITO on Fl-OSCs, let alone the foldable solar cells, where flexible electrodes for lightweight, wearable, foldable, and stretchable products are highly demanding (Park et al., 2018; Jinno et al., 2017; Kang et al., 2015; Zhao et al., 2017). In recent years, a number of emerging flexible transparent electrodes (FTEs) such as graphene, metal nanowires, conducting polymers (CPs), and thin metals have been studied (Park et al., 2014; Xia et al., 2012; Zhao et al., 2015; Jeon et al., 2015; Seo et al., 2017; Yang et al., 2017; Lu et al., 2017; Huang et al., 2015; Liu et al., 2017). Still, each of these FTEs unveils problems such as high cost, difficulty in mass production, lack of reproducibility, inferior toughness, etc, resulting in their incompatibility with Fo-OSC. These obstacles need to be hurdled before the further implementations of Fo-OSCs in practical applications (Cheng et al., 2016b, 2016a; Fan et al., 2016; Wang et al., 2017).

Among these FTEs, poly(3,4-ethylenedioxythiophene):poly(styrenesulfonate) (PEDOT:PSS) has been extensively used because it offers an extremely uniform and smooth film with highly intrinsic transparency

[1]Ningbo Institute of Materials Technology and Engineering, Chinese Academy of Sciences, Ningbo, 315201, China

[2]Center of Materials Science and Optoelectronics Engineering, University of Chinese Academy of Sciences, Beijing 100049, China

[3]Department of Chemistry, Northwestern University, 2145 Sheridan Road, Evanston, IL 60208, USA

[4]Lead Contact

*Correspondence: geziyi@nimte.ac.cn

https://doi.org/10.1016/j.isci.2020.100981

in the visible-light region, good compatibility with roll-to-roll printing, and low-cost solution processability (Vosgueritchian et al., 2012; Worfolk et al., 2015; Kim et al., 2011; Xia et al., 2012; Gupta et al., 2013; Zhao et al., 2016; Wang et al., 2018; Chen et al., 2019). To date, high figure-of-merit (FoM) PEDOT:PSS films prepared through doping treatments (such as dimethyl sulfoxide (DMSO), ethylene glycol (EG), and ZonylFS300) (Vosgueritchian et al., 2012) and surface infiltration treatments, namely post-treatments, with $H_2SO_4$, $HNO_3$, $H_3PO_4$, etc, have been reported (Xia et al., 2012; Yeon et al., 2015; Meng et al., 2015). For instance, Ouyang group has reported high conducting PEDOT:PSS films with $H_2SO_4$ treatment (Xia et al., 2012; Kim et al., 2015). Lim group has also reported that the conductivity of PEDOT:PSS could reach about 3964 S/cm via post-treatment with $HNO_3$ (Yeon et al., 2015). Similarly, Zhou group has reported a high PEDOT:PSS films through $H_3PO_4$ treatment (Meng et al., 2015). However, all these acids are highly corrosive, which could easily damage the plastic substrates such as PET, and harmful to health and environment. Therefore, these processing methods are not suitable for the sustainable development of flexible electronic devices in the future. Due to this, the preparation of flexible and durable plastic electrode with high FoM and good environmental friendliness as well as excellent foldability still remained as a significant challenge.

Here, we demonstrate highly efficient Fo-OSCs fabricated on a modified PEDOT:PSS (m-PEDOT:PSS)/polyethylene terephthalate (PET) substrate by polyhydroxy compound (D-sorbitol) micro-doping PEDOT:PSS followed by an eco-friendly acid treatment with citric acid, malic acid, or tartaric acid, respectively. The polyhydroxy compound micro-doping improves the interfacial adhesion of PEDOT:PSS to the PET substrate through a strong hydrogen bond and van der Waals bond affinity and reduces the interfacial mechanical wear. As an alternative to strong corrosive acid, the eco-friendly acids can be easily extracted from green fruits and are harmless to health and the environment, which are thus more suitable for the future large-scale manufacturing of OSCs. Owing to its excellent FoM, superior mechanical flexibility and long-term air stability of the eco-friendly acid-treated m-PEDOT:PSS, the Fo-OSC device is able to produce a high-power conversion efficiency (PCE) of 14.17%. In addition, after 1,000 cycles of continuous bending test or persistent folding, the flexible device still retained over 90% or 80% of the initial PCE, respectively. To the best of our knowledge, this is the highest PCE for folding-flexible OSCs reported so far. For the first time, this work demonstrates that these eco-friendly acid-treated m-PEDOT:PSS FTEs have great potentials for the eco-friendly fabrication of highly efficient Fo-OSCs for future commercial applications in wearable and portable devices.

## RESULTS AND DISCUSSION

### Optical and Electrical Characteristics of PEDOT:PSS

Three green-acid-impregnated as-cast PEDOT:PSS films were selected to precisely adjust the curing concentration of the acid treatment to produce PEDOT:PSS electrodes with high FoM. These three eco-friendly acids can be easily extracted from lemons, apples, and grapes by industrial methods, namely citric acid, tartaric acid, and malic acid (the molecular structure as shown in Figure 1A), respectively. Figure 1C plots the square resistance ($R_{sq}$) values of the PEDOT:PSS films with different kinds and concentrations of acids. The conductivity of PEDOT:PSS films with various eco-friendly acid treatment are shown in Figure S3. Obviously, the film treated with citric acid at 58 wt.% achieves the highest conductivity (1960 S/cm) and the lowest $R_{sq}$ (~93 $\Omega sq^{-1}$). All $R_{sq}$ of the treated PEDOT:PSS films decreases as the concentration of the three acids increases. Because of the difference in the number of hydrophilic terminal (hydroxyl groups and carboxyl groups), the saturation of citric acid, tartaric acid, and malic acid in deionized water are approximately 58 wt. %, 58 wt. %, and 52 wt. %, individually. Figures 1B and S1 show the transmittance spectra of the PEDOT:PSS films with different eco-friendly acid treatment. Obviously, the PEDOT:PSS films with optimum transmittance is obtained by citric acid treatment due to the removal of a large amount of PSS components and a better crystallinity of PEDOT. Among these eco-friendly acids, the saturate concentration of acid depends on the number of hydrophilic groups, and the carboxyl groups can better induce the conformational change of PEDOT from the coil to extended-coil or linear nanofibrils structure. Consequently, it results in a more delocalized positive charge on PEDOT. It can be seen that the PEDOT:PSS films with the three eco-friendly acid treatments exhibit a broad plateau above 85.0% in the visible and near-infrared regions, endowing them good candidates for the transparent conductive electrodes of OSCs. In addition, FoM is a more comprehensive parameter for evaluating the performance of flexible electrodes, where higher FoM values always correspond to better optoelectronic properties of FTEs. The FoM for transparent

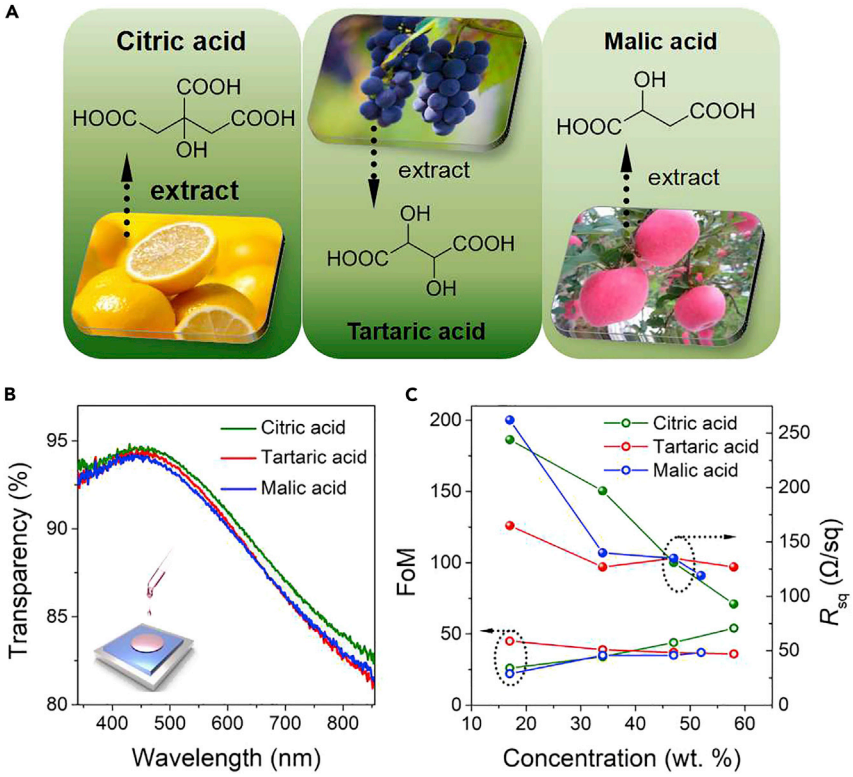


**Figure 1. Optoelectrical Performance of PEDOT:PSS Electrodes**

(A) Molecular structures of citric acid, tartaric acid, and malic acid, respectively.

(B and C) (B) Transmittance spectrum. (C) $R_{sq}$ and FoM of the PEDOT:PSS films with the three eco-friendly acids treatments at different concentrations

conductors is defined as the ratio of direct current conductivity ($\sigma_{dc}$) to optical conductivity ($\sigma_{op}$) (Vosguer-itchian et al., 2012):

$$\mathrm{FoM} = \frac{\sigma_{dc}}{\sigma_{op(\lambda)}} = \frac{188.5}{R_{sq}\left(T_{(\lambda)}^{-0.5} - 1\right)} \qquad \text{(Equation 1)}$$

where $\lambda$ is the wavelength of light at which the transmittance is measured (typically 550 nm) and $R_{sq}$ is the square resistance. Typically, FoM greater than 35 is the minimum benchmark for indicating the commercial viability of a transparent conductor (Worfolk et al., 2015). Figure 1C plots the FoM values of the three green acid-treated PEDOT:PSS films. The FoM of citric-acid-treated PEDOT:PSS films is the highest among the three acid-treated films, exceeding 35 and up to 54. Meanwhile, the FoM of tartaric-acid- and malic-acid-treated PEDOT:PSS films reaches 39 and 34, respectively, which is greater than the minimum benchmark for indicating the commercial viability of a transparent conductors. Table S1 summarizes the conductivities and $R_{sq}$ of various acid-treated PEDOT:PSS films. It is well known that some strong and corrosive inorganic acids, such as $H_2SO_4$, $HNO_3$, and $H_3PO_4$, can improve their conductivity by removing PSS from PEDOT:PSS, but these strong inorganic acids could easily severely damage the plastic substrates such as PET, and be harmful to the environment and human body. To this end, eco-friendly and low-cost acid extracted from fruits can be utilized as a substitute to the strong and corrosive inorganic acids to improve the conductivity of PEDOT:PSS for its application of transparent electrodes in OSCs.

## Transmittance and Morphology Investigations of PEDOT:PSS

Considering that the sunlight is absorbed and utilized by the photoactive layer, it primarily passes through the transparent anode, so it is critical to ensure high transmittance and low resistance. Figures 2A, 2D, and S3 shows the transmittance spectra, average transmittance, $R_{sq}$, and conductivity of PEDOT:PSS electrodes with common various acids treatment (data summarized in Table S1). ITO/PET shows poorest transmittance

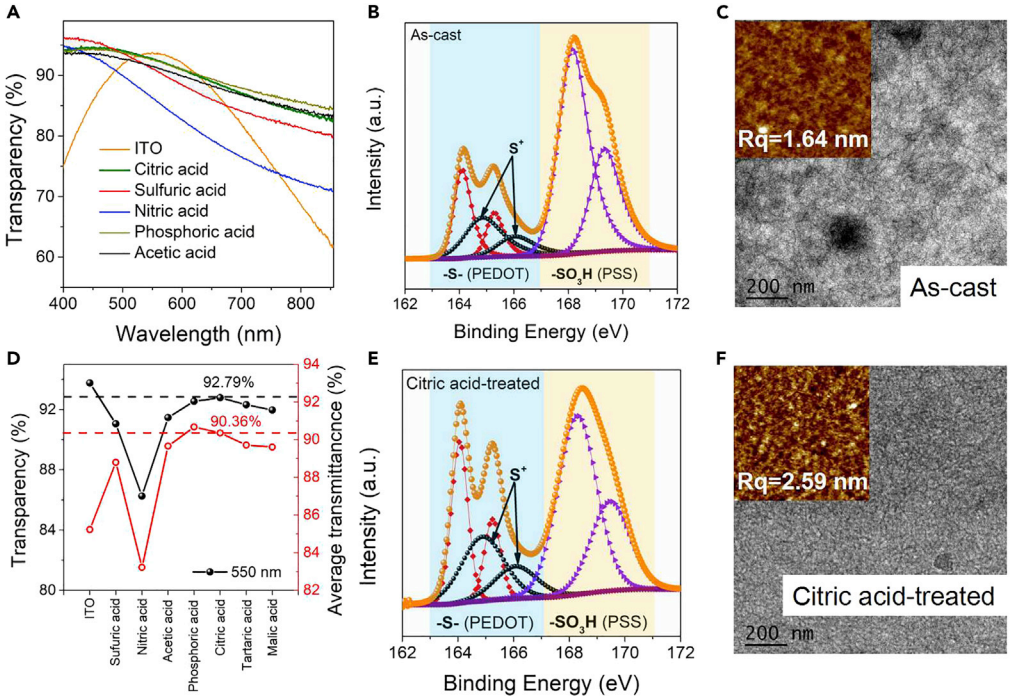


**Figure 2. Transmittance and Morphological Characteristics of FTEs**

(A) Transmittance spectrum of ITO/PET and PEDOT:PSS with various acid treatment.

(D) Comparison of the transmittance at 550 nm and average transmittance of various transparent electrodes.

(B and E) Fitted S 2pXPS spectra: (B) as-cast films, (E) the films with optimal concentration citric acid treatments.

(C and F) TEM images of the (C) pristine, (F) citric-acid-treated PEDOT:PSS films on PET plastic substrates. The insets: AFM images corresponding to PEDOT:PSS films. Scale bar: 2 × 2 $\mu m^2$.

properties, especially low in the shorter (<450 nm) and higher wavelength region (>650nm). Even without considering its inherent physical properties of being rigid, bulky, and fragile, such low transmittance in the major absorbing region makes ITO an unsuitable alternative for the preparation of highly efficient Fl-OSCs. Highly conductive PEDOT:PSS transparent electrodes have been reported by acid treatment, such as sulfuric acid, nitric acid, phosphoric acid, etc. (Kim et al., 2014;Meng et al., 2015). Although nitric acid and sulfuric acid treatment can obtain high conductivity, PEDOT often rearranges and crystallizes due to its strong acidity, causing poor transmissivity of electrodes. In addition, powerful oxidizing properties can also severely destroy the plastic substrates, making them unsuitable for preparing high-efficiency Fl-OSCs. Phosphoric-acid- and acetic-acid-treated PEDOT:PSS films can obtain better transmittance, but its poor conductivity hinders its application a high-quality transparent electrode for the flexible photovoltaic cells (as shown in Figure S3). High-quality FTEs based on eco-friendly acids exhibit excellent optoelectronic performance (high conductivity and transmittance) and good compatibility, protecting the plastic underlying substrates, which is an effective way toward realizing highly efficient and flexible OSCs.

To investigate the surface morphological features of the green-acid-treated PEDOT:PSS films, transmission electron microscope (TEM) and atomic force microscopy (AFM) were conducted. Figures 2C and 2F show the TEM image of the PEDOT:PSS films treated without and with citric acid, and insets are AFM image of the corresponding sample. As-cast PEDOT:PSS film exhibits coiled structures with no obvious aggregation. When highly concentrated green acid is dropped on the as-cast PEDOT:PSS film, $H^+$ from the acids will associate with the $PSS^-$ to form neutral PSSH in the PEDOT:PSS films (Xia et al., 2012; Li et al., 2015; Kaltenbrunner et al., 2012). These PSSH chains are neutral and, therefore, do not have any Columbic interactions with PEDOT in the films. As a result, PSSH chains are segregated away from the films matrix, which becomes the major reason of the larger phase separation in the eco-friendly acid-treated PEDOT:PSS films compared with the as-cast film. Furthermore, these PSSH chains can be removed from the films through washing, which reduces the energy barrier width for inter-chain and inter-domain charge hopping. In addition, PEDOT by nature has a coil conformation as a result of the coiled $PSS^-$ conformation and the

Columbic interactions between $PSS^-$ and the positively charged PEDOT in the as-cast PEDOT:PSS films. The disappearance of the Columbic interaction due to the formation of PSSH in the green acid-treated PEDOT:PSS films has also induced the conformational change of PEDOT from the coil to extended-coil or linear nanofibrils structure (as shown in Figure 2F), which results in a more delocalized positive charge on PEDOT. Both the conformational change and the removal of PSSH have led to the conductivity improvement of the film. This observation is consistent with the AFM results, where the root-mean-square (RMS) roughness of pristine film (1.64 nm) was increased to 2.59 nm due to citric acid treatment. Tartaric-acid- and malic-acid-treated PEDOT:PSS films exhibited a similar phase separation with RMS roughness as high as 2.74 nm and 2.52 nm, respectively (as shown in Figure S5).

The atomic contents and elemental states of the PEDOT:PSS films were conducted by X-ray photoelectron spectroscopy (XPS) measurement. Figures 2B, 2E, and S6 show the S 2p X-ray photoelectron spectroscopy (XPS) of the as-cast film and the films with the three acid treatments. It illustrates the S 2p photoelectron peaks consisting of the spin-split doublet (S 2p 1/2 and S 2p 3/2) for which relative intensity ratio was 1:2. Notably, the XPS bands between 167 and 171 eV are mainly originated from the sulfonate moieties ($–SO_3H$) of PSS, whereas, the XPS bands between 161 and 167 eV are mainly originated from thiophene rings (–S–) of PEDOT(Kim et al., 2014). The fitted peaks colored in black correspond to the $S^+$ in the PEDOT:PSS films. Our curve fitting results show that the PSSH peak intensity was significantly reduced for the three acid-treated samples, which indicates that some PSSH was significantly removed upon the three acid treatments on PEDOT:PSS (Zhang et al., 2013, 2017). These results are responsible for the improved FoM of PEDOT:PSS. It was found that the removal of a large amount of PSS components from the PEDOT:PSS matrix resulted in the structural rearrangement of PEDOT with enhanced crystallinity. It is widely acknowledged that crystalline order in CPs facilitates an efficient intra- and inter-chain charge transport, resulting in a highly conducting state (Kim et al., 2014). Figure S7 presents the energy dispersive spectrometer (EDS) elemental mapping distribution of the S element in the pristine PEDOT:PSS film and the films treated with three eco-friendly acids. EDS shows that the S element distribution of pristine PEDOT:PSS film is relatively dense, whereas the distribution of S elements in the film after three eco-friendly acid treatments is rare, which is in accordance with the XPS test results.

### Physical Properties of PEDOT:PSS Films

For making high-quality FTEs, it is necessary to have the optimal bending properties without reducing the transparency and conductivity of the electrode. Acid treatment of the PEDOT:PSS films will greatly increase the conductivity of the films but will reduce the flexibility of the films at the mean time. Harsh bending deformation may cause crack propagation in the acid-treated PEDOT:PSS films, resulting in a stark increase in the films resistance, thus affecting the bending and folding properties of the electrode and the resulted OSCs. The issue can be circumvented by adding an appropriate amount of D-sorbitol to the PEDOT:PSS to increase the adhesion of the PEDOT:PSS solution and strengthen the interface bonding between the FTEs and PET substrate, thereby increasing the flexibility of the PEDOT:PSS films. Figure 3A shows the schematic illustration of the hydrogen bond and the van der Waals bond effect that would provide a somewhat stronger adhesion of PEDOT:PSS films on PET, thus obtaining a high-quality FTE. To investigate the interface bonding interactions between the PEDOT:PSS and plastic substrate, the monitoring on the adhesive force was conducted, as depicted in Figure 3B. Pure PEDOT:PSS solution has a relatively low adhesion force of 0.084 mN. When a proper amount of polyhydroxy compound is added to the PEDOT:PSS solution, the adhesion force of the PEDOT:PSS solution can be significantly improved to 0.182 mN, so that a transparent electrode with high mechanical properties can be obtained.

High-quality FTEs should retain most of its initial conductivity when subjected to bending and folding deformation. Figure 3C shows the variation of $R_{sq}$ of m-PEDOT:PSS/PET with bending radius ($r$) of 4 mm and citric-acid-treated PEDOT:PSS/PET (control sample) with folding as a function of the number of bending cycles. The conductivity of the m-PEDOT:PSS film made by doping a small amount of polyhydroxy compound in PEDOT:PSS is not deteriorated. Our bending study shows that two samples based on m-PEDOT:PSS/PET and PEDOT:PSS/PET retained a lower $R_{sq}$ when they are subsequently relaxed after 1,000 cycles of bending ($r$: 4.0 mm), which is increased by 4% and 13% compared with the initial value, respectively. For the folding bending, the two samples increased by 24% and 44% in $R_{sq}$, respectively, which indicates that the incorporation of polyhydroxy compound increases the toughness of the PEDOT:PSS film and its adhesion to the PET substrate. Thereby, the film can maintain high electrical conductivity under large mechanical changes.

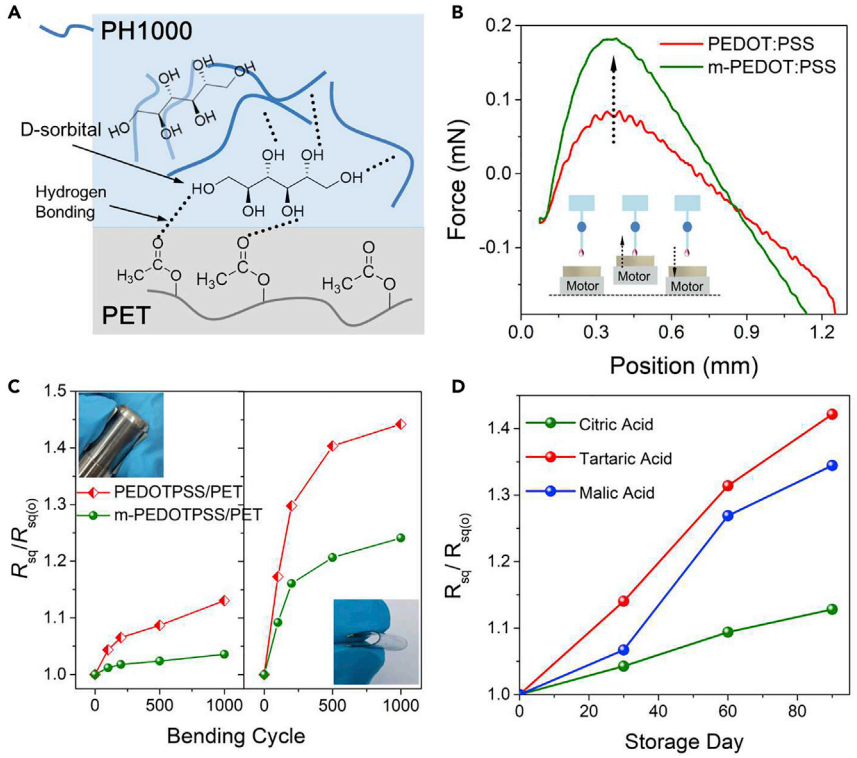


**Figure 3. Mechanical Properties and Air-Stability of PEDOT:PSS Electrodes**

(A) Schematic illustration of the increase in mechanical flexibility of PEDOT:PSS/PET with polyhydroxy compound.

(B) Adhesive force of pure PEDOT:PSS solution and PEDOT:PSS solution doped with 5% D-sorbitol (inset is the schematic of the process for adhesion force measurement).

(C) $R_{sq}/R_{sq(o)}$ of PEDOT:PSS/PET and m-PEDOT:PSS (doped with polyhydroxy compound)/PET as a function of bending cycles.

(D) $R_{sq}/R_{sq(o)}$ variation of m-PEDOT:PSS/PET with three eco-friendly acid treatments as a function of storage days in air.

PEDOT: PSS film can easily absorb moisture in a humid environment; it is possible to make the conductive polymer susceptible to moisture and affect the charge jump of the PEDOT:PSS film, thereby reducing the conductivity. Therefore, we further investigated the air stability of PEDOT:PSS/PET samples with three eco-friendly acid treatment exposed to ambient air (temperature: 10°C –20°C; humidity: 50%–65%). Figure 3D shows $R_{sq}/R_{sq(o)}$ variation of m-PEDOT:PSS/PET with three eco-friendly acid treatments within a three-month period. An increase of 10% in $R_{sq}$ is observed for the m-PEDOT:PSS films that are treated with citric acid. The other two acid-treated m-PEDOT:PSS films have a larger increase of 33%–40% in $R_{sq}$. Although PEDOT:PSS film storage conditions are harsh and sensitive, the limited increase in $R_{sq}$ of m-PEDOT:PSS/PET indicates that PEDOT:PSS has good air stability.

## Device Performance

On the basis of the PEDOT:PSS/PET substrates, we fabricated Fo-OSC with a structure of PET/m-PEDOT:PSS FTE/PEDOT:PSS (4083)/photoactive layer/perylenediimide functionalized with amino N-oxide (PDINO)/Al (as shown in Figure 4A). The photoactive layer consists of a mixture of electron donor poly [4,8-bis(5-(2-ethylhexyl)4-fluorothiophen-2-yl) benzo[1,2-b:4,5-b']-dithiophene-alt1,3-bis(thiophen-2-yl)-5,7-bis(2-ethylhexyl)benzo-[1,2-c:4,5-c']-dithiophene-4,8-dione] (PBDB-T-2F) and electron acceptor 2,20-((2Z,20Z)-((12,13-bis(2ethylhexyl)-3,9-diundecyl-12,13-dihydro-[1,2,5] thiadiazolo[3,4-e]thieno[2,"30':4',50] thieno[20,30:4,5] pyrrolo[3,2-g]thieno[20,30:4,5]thieno[3,2-b]indole-2,10-diyl)bis(methanylylidene))bis(5,6-difluoro-3-oxo-2,3-dihydro-1H-indene-2,1-diylidene)) dimalononitrile (Y6) (Zhang et al., 2018; Li et al., 2018). Figure S8 shows the molecular structures of PBDB-T-2F, Y6, PDINO, and PEDOT:PSS, respectively. The energy level alignment of the components of the flexible devices is shown in Figure S9.

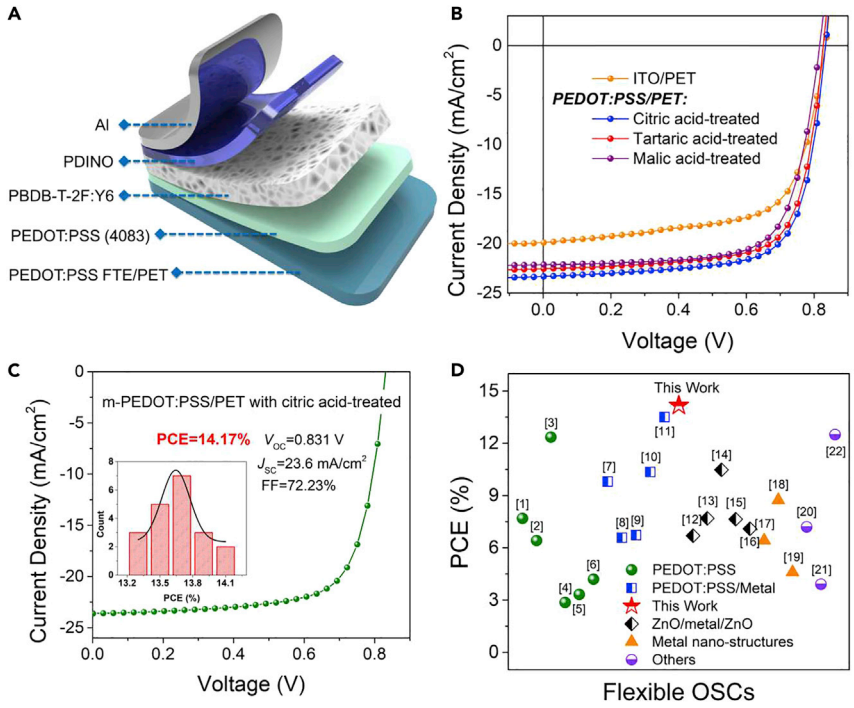


**Figure 4. Photovoltaic Characteristics of Folding-Flexible OSCs**

(A) Device structure of the flexible OSC.

(B) *J–V* characteristics of flexible OSCs fabricated on ITO/PET and PEDOT:PSS/PET with three eco-friendly acid treatments.

(C) Optimal *J–V* characteristics of flexible OSCs fabricated on m-PEDOT:PSS/PET with citric acid treatments (insert is corresponding histogram distribution of PCE counts for 20 individual devices).

(D) Recent scatterplot report for PCE values of flexible OSCs, all references are listed in Supplemental Information.

In order to evaluate the performance of Fo-OSC, control devices with ITO (=120 nm)/glass were first fabricated with efficiency of 15.41%. Figure 4B shows the current density–voltage (*J–V*) curves of flexible devices fabricated on ITO/PET and PEDOT:PSS/PET substrates with three eco-friendly acid treatment. Note that the PEDOT:PSS/PET electrode was prepared by spin coating PEDOT:PSS on PET followed by a subsequent green acid treatment under optimized concentration. Flexible devices of PEDOT:PSS with citric acid, tartaric, and malic acid treatment exhibit an efficiency of 13.94%, 13.47%, and 12.90%, respectively, consistent with the optical performance of the corresponding electrode. Table 1 summarizes the photovoltaic performance data of all the flexible OSC devices. Figure 4C reveals the *J–V* test result of the prepared optimal Fl-OSCs based on citric-acid-treated m-PEDOT:PSS/PET. The folding-flexible devices yielded the best PCE of 14.17% with $V_{OC}$ of 0.831 V, $J_{SC}$ of 23.60 mA cm$^{-2}$, and FF of 72.23%, which is the highest value reported so far for Fl-OSCs (as shown in Figure 4D and Table S2). Inset is the corresponding histogram distribution of PCE counts for 20 individual devices. Unfortunately, the reference solar cells based on ITO/PET exhibited a low initial PCE of 11.03%, which was mainly caused by the low-quality sputtering that yielded a relatively low optical transparency, especially low in the shorter (<450 nm) and higher wavelength region (>650nm), and high reflectivity (see Figures 2A and S2), implying a promising replacement of ITO by the eco-friendly acid-treated PEDOT:PSS electrode. The external quantum efficiency (EQE) spectra of the rigid and flexible OSCs are shown in Figure S10. EQE spectrum of the m-PEDOT:PSS/PET-based flexible device has a higher peak in the wavelength range from 320 to 420 nm compared with the ITO/glass-based reference device. Conventional ITO/glass transparent electrodes have a strong reflectance at near-ultraviolet wavelengths, thus limiting the absorption of active layer in this wavelength range (as shown in Figure S2).

## Bending Performance of Flexible Devices

In order to compare the bending flexibility of these flexible devices, the bending test was carried out in a nitrogen-filled glove box without encapsulation. These devices were bent on a cylinder with a radius of

| Devices | $V_{oc}$ [V] | $J_{sc}$ [mA cm$^{-2}$] | FF [%] | PCE (ave.[a]) [%] |
|---|---|---|---|---|
| ITO (110 nm)/Glass | 0.841 | 25.37 | 72.26 | 15.41 (15.02) |
| PEDOT:PSS/PET[b] | 0.834 | 23.29 | 71.79 | 13.94 (13.51) |
| PEDOT:PSS/PET[c] | 0.827 | 22.53 | 72.28 | 13.47 (13.23) |
| PEDOT:PSS/PET[d] | 0.816 | 22.12 | 71.45 | 12.90 (12.78) |
| m-PEDOT:PSS/PET | 0.831 | 23.60 | 72.23 | 14.17 (13.73) |
| ITO (120 nm)/PET | 0.833 | 19.78 | 66.88 | 11.03 (10.83) |

**Table 1. Photovoltaic Performances of Flexible Devices Based on PEDOT:PSS Films and ITO**

[a]Average PCE of 20 individual devices.

[b]Citric-acid-treated PEDOT:PSS electrodes.

[c]Tartaric-acid-treated PEDOT:PSS electrodes.

[d]Malic-acid-treated PEDOT:PSS electrodes.

4 mm. Figure 5A shows the change in normalized PCEs of the three flexible devices in a continuous bending test. Our results show that the Fo-OSC with m-PEDOT:PSS/PET maintains a high efficiency without significant reduction after 500 bending cycles. In addition, this device still maintains over 90% of the original PCE even after 1,000 bending cycles. Meanwhile, flexible device based on PEDOT:PSS/PET substrate is able to retain about 88% of the original PCE value after 1,000 bending cycles. In contrast, after 1,000 cycles of bending, the PCE of ITO-based flexible device has dropped dramatically due to the intrinsic fragility of the sputtered ITO films, maintaining only 47% of the original PCE. The trend for PCE in the bending test indicates that the incorporation of polyhydroxy compound significantly improves the mechanical flexibility of the flexible ITO-free OSC devices.

In order to investigate the mechanical folding performance of the Fl-OSCs based on m-PEDOT:PSS/PET, the device is to be subjected to folding to induce vertical creases. Figure 5B shows the change in normalized PCEs of flexible devices when subjected to folding. As depicted in the figure, the efficiency of flexible solar cells with m-PEDOT:PSS/PET is significantly reduced when folded five to ten times. However, after being folded 1,000 times, the flexible devices still maintained a reasonable PCE of 83% (mid-device folding) and 73% (Al top electrode folding). The mechanical flexibility of the device is mainly attributed to the fact that the incorporation of polyhydroxy compound in PEDOT:PSS can improve the adhesion of PEDOT:PSS solution (see Figure 3B), so that PEDOT:PSS can be well combined with the PET plastic substrate, thereby improving the robustness of PEDOT:PSS electrode. In addition, the low $R_{sq}$ value imparted by the continuous conductive path on the polyhydroxy compound also contributes to the improved flexibility of the electrode. Overall, our results highlight the importance of polyhydroxy compound for high-performance Fo-OSC.

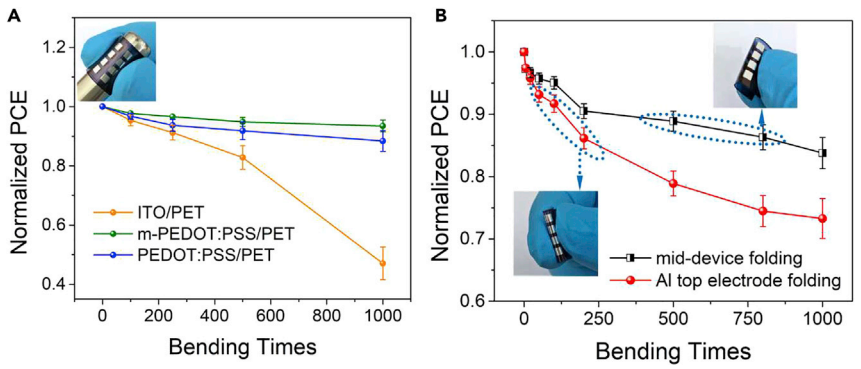


**Figure 5. Mechanical Flexibility of OSCs**

(A) Changes in normalized PCEs of the flexible devices based on ITO/PET and citric-acid-treated m-PEDOT:PSS/PET and PEDOT:PSS/PET in a continuous bending test.

(B) Changes in normalized PCEs of optimal flexible device based on citric-acid-treated m-PEDOT:PSS/PET electrode with mid-device and Al top electrode folding.

## Conclusions

In summary, we have demonstrated a highly efficient and folding-flexible OSC fabricated on m-PEDOT:PSS/PET substrates with environment-friendly acid treatment. Through doping of polyhydroxy compound and treatment with eco-friendly acid, it has endowed the m-PEDOT:PSS electrode to be resilient to severe bending and folding deformation, exhibiting a high FoM of 54, an excellent mechanical flexibility and foldability as well as a long-term air stability. Thus, the green-acid-treated folding-flexible OSCs showed a high PCE of 14.17%, $V_{OC}$ of 0.831 V, $J_{SC}$ of 23.60 mA $cm^{-2}$, and FF of 72.23% with an excellent folding flexibility. Our work opens a new avenue to the investigation of the low-cost eco-friendly acid-treated PEDOT:PSS flexible transparent electrodes for further implementation of wearable, foldable, and cost-effective OSCs, which are of great potential to promote the commercialization of OSCs.

## METHODS

All methods can be found in the accompanying Transparent Methods supplemental file.

## SUPPLEMENTAL INFORMATION

Supplemental Information can be found online at https://doi.org/10.1016/j.isci.2020.100981.

## ACKNOWLEDGMENTS

This work was financially supported by the National Key R&D Program of China (2017YFE0106000), National Natural Science Foundation of China (51773212, 21574144, 21674123 and 61705240), the National Science Fund for Distinguished Young Scholars (21925506), Zhejiang Provincial Natural Science Foundation of China (LR16B040002), Ningbo S&T Innovation 2025 Major Special Programme (2018B10055), Ningbo Municipal Science and Technology Innovative Research Team (2015B11002 and 2016B10005), CAS Key Project of Frontier Science Research (QYZDB-SSW-SYS030), and CAS Key Project of International Cooperation (174433KYSB20160065).

## AUTHOR CONTRIBUTIONS

W.S. performed the fabrication and characterization of folding-flexible solar cells, including optical and electrical characterization, adhesion test, stability test, and flexing tests of PEDOT:PSS films. W.S. also conducted the data analysis. R.P. conducted the XPS data analysis. L.K.H. and R.P. conducted the EDS data analysis. B.F. and J.G. performed the AFM measurement and analyzed the results. C.L., L.H., and T.L. provided feedbacks regarding overall data analysis. The project was supervised and directed by Z.G.. W.S. wrote the manuscript with large contributions from B.F., R.P., L.K.H., A.F., and Z.G.. All authors commented on the manuscript for improvements.

## DECLARATION OF INTERESTS

The authors declare no competing financial interest.

Received: November 23, 2019
Revised: December 25, 2019
Accepted: March 7, 2020
Published: April 24, 2020

## REFERENCES

Baran, D., Ashraf, R.S., Hanifi, D.A., Abdelsamie, M., Gasparini, N., Rohr, J.A., Holliday, S., Wadsworth, A., Lockett, S., Neophytou, M., et al. (2017). Reducing the efficiency-stability-cost gap of organic photovoltaics with highly efficient and stable small molecule acceptor ternary solar cells. Nat. Mater. *16*, 363–369.

Chen, R., Sun, K., Zhang, Q., Zhou, Y., Li, M., Sun, Y., Wu, Z., Wu, Y., Li, X., Xi, J., et al. (2019). Sequential solution polymerization of poly(3,4-ethylenedioxythiophene) using $V_2O_5$ as oxidant for flexible touch sensors. iScience *12*, 66–75.

Cheng, T., Zhang, Y.-Z., Yi, J.-P., Yang, L., Zhang, J.-D., Lai, W.-Y., and Huang, W. (2016b). Inkjet-printed flexible, transparent and aesthetic energy storage devices based on PEDOT:PSS/Ag grid electrodes. J. Mater. Chem. A *4*, 13754–13763.

Cheng, T., Zhang, Y.-Z., Zhang, J.-D., Lai, W.-Y., and Huang, W. (2016a). High-performance free-standing PEDOT:PSS electrodes for flexible and transparent all-solid-state supercapacitors. J. Mater. Chem. A *4*, 10493–10499.

Fan, X., Xu, B., Liu, S., Cui, C., Wang, J., and Yan, F. (2016). Transfer-printed PEDOT:PSS electrodes using mild acids for high conductivity and improved stability with application to flexible organic solar cells. ACS Appl. Mater. Interfaces *8*, 14029–14036.

Gupta, D., Wienk, M.M., and Janssen, R.A.J. (2013). Efficient polymer solar cells on opaque substrates with a laminated PEDOT:PSS top electrode. Adv. Energy Mater. *3*, 782–787.

Huang, J., Li, C.-Z., Chueh, C.-C., Liu, S.-Q., Yu, J.-S., and Jen, A.K.Y. (2015). 10.4% Power conversion efficiency of ITO-free organic

photovoltaics through enhanced light trapping configuration. Adv. Energy Mater. *5*, 1500406.

Jeon, I., Cui, K., Chiba, T., Anisimov, A., Nasibulin, A.G., Kauppinen, E.I., Maruyama, S., and Matsuo, Y. (2015). Direct and dry deposited single-walled carbon nanotube films doped with MoOx as electron-blocking transparent electrodes for flexible organic solar cells. J. Am. Chem. Soc. *137*, 7982–7985.

Jinno, H., Fukuda, K., Xu, X., Park, S., Suzuki, Y., Koizumi, M., Yokota, T., Osaka, I., Takimiya, K., and Someya, T. (2017). Stretchable and waterproof elastomer-coated organic photovoltaics for washable electronic textile applications. Nat. Energy *2*, 780–785.

Kaltenbrunner, M., White, M.S., Glowacki, E.D., Sekitani, T., Someya, T., Sariciftci, N.S., and Bauer, S. (2012). Ultrathin and lightweight organic solar cells with high flexibility. Nat. Commun. *3*, 770.

Kang, H., Jung, S., Jeong, S., Kim, G., and Lee, K. (2015). Polymer-metal hybrid transparent electrodes for flexible electronics. Nat. Commun. *6*, 6503.

Kim, Y.H., Sachse, C., Machala, M.L., May, C., Müller-Meskamp, L., and Leo, K. (2011). Highly conductive PEDOT:PSS electrode with optimized solvent and thermal post-treatment for ITO-free organic solar cells. Adv. Funct. Mater. *21*, 1076–1081.

Kim, J.K., Kim, W., Wang, D.H., Lee, H., Cho, S.M., Choi, D.G., and Park, J.H. (2013). Layer-by-layer all-transfer-based organic solar cells. Langmuir *29*, 5377–5382.

Kim, N., Kee, S., Lee, S.H., Lee, B.H., Kahng, Y.H., Jo, Y.R., Kim, B.J., and Lee, K. (2014). Highly conductive PEDOT:PSSnanofibrils induced by solution-processed crystallization. Adv. Mater. *26*, 2268–2272.

Kim, N., Kang, H., Lee, J.H., Kee, S., Lee, S.H., and Lee, K. (2015). Highly conductive all-plastic electrodes fabricated using a novel chemically controlled transfer-printing method. Adv. Mater. *27*, 2317–2323.

Li, Z., Qin, F., Liu, T., Ge, R., Meng, W., Tong, J., Xiong, S., and Zhou, Y. (2015). Optical properties and conductivity of PEDOT:PSS films treated by polyethylenimine solution for organic solar cells. Org. Electron. *21*, 144–148.

Li, W., Ye, L., Li, S., Yao, H., Ade, H., and Hou, J. (2018). A high-efficiency organic solar cell enabled by the strong intramolecular electron push-pull effect of the nonfullerene acceptor. Adv. Mater *30*, 1707170.

Ling, H., Liu, S., Zheng, Z., and Yan, F. (2018). Organic flexible electronics. Small Methods *2*, 1800070.

Liu, Q., Toudert, J., Ciammaruchi, L., Martínez-Denegri, G., and Martorell, J. (2017). High open-circuit voltage and short-circuit current flexible polymer solar cells using ternary blends and ultrathin Ag-based transparent electrodes. J. Mater. Chem. A *5*, 25476–25484.

Lu, S., Lin, J., Liu, K., Yue, S., Ren, K., Tan, F., Wang, Z., Jin, P., Qu, S., and Wang, Z. (2017). Large area flexible polymer solar cells with high efficiency enabled by imprinted Ag grid and modified buffer layer. Acta Mater. *130*, 208–214.

Meng, W., Ge, R., Li, Z., Tong, J., Liu, T., Zhao, Q., Xiong, S., Jiang, F., Mao, L., and Zhou, Y. (2015). Conductivity enhancement of PEDOT:PSS films via phosphoric acid treatment for flexible all-plastic solar cells. ACS Appl. Mater. Interfaces *7*, 14089–14094.

Min, X., Jiang, F., Qin, F., Li, Z., Tong, J., Xiong, S., Meng, W., and Zhou, Y. (2014). Polyethylenimine aqueous solution: a low-cost and environmentally friendly formulation to produce low-work-function electrodes for efficient easy-to-fabricate organic solar cells. ACS Appl. Mater. Interfaces *6*, 22628–22633.

Park, H., Chang, S., Zhou, X., Kong, J., Palacios, T., and Gradecak, S. (2014). Flexible graphene electrode-based organic photovoltaics with record-high efficiency. Nano Lett. *14*, 5148–5154.

Park, S., Heo, S.W., Lee, W., Inoue, D., Jiang, Z., Yu, K., Jinno, H., Hashizume, D., Sekino, M., Yokota, T., et al. (2018). Self-powered ultra-flexible electronics via nano-grating-patterned organic photovoltaics. Nature *561*, 516–521.

Peng, R., Song, W., Yan, T., Fanady, B., Li, Y., Zhan, Q., and Ge, Z. (2019). Interface bonding engineering of a transparent conductive electrode towards highly efficient and mechanically flexible ITO-free organic solar cells. J. Mater. Chem. A *7*, 11460–11467.

Qian, D., Zheng, Z., Yao, H., Tress, W., Hopper, T.R., Chen, S., Li, S., Liu, J., Chen, S., Zhang, J., et al. (2018). Design rules for minimizing voltage losses in high-efficiency organic solar cells. Nat. Mater. *17*, 703–709.

Seo, J.H., Hwang, I., Um, H.D., Lee, S., Lee, K., Park, J., Shin, H., Kwon, T.H., Kang, S.J., and Seo, K. (2017). Cold isostatic-pressured silver nanowire electrodes for flexible organic solar cells via room-temperature processes. Adv. Mater. *29*, 1701479.

Søndergaard, R., Hösel, M., Angmo, D., Larsen-Olsen, T.T., and Krebs, F.C. (2012). Roll-to-roll fabrication of polymer solar cells. Mater. Today *15*, 36–49.

Song, W., Fan, X., Xu, B., Yan, F., Cui, H., Wei, Q., Peng, R., Hong, L., Huang, J., and Ge, Z. (2018). All-solution-processed metal-oxide-free flexible organic solar cells with over 10% efficiency. Adv. Mater. *30*, e1800075.

Song, W., Li, W., Peng, R., Fanady, B., Huang, J., Zhu, W., Xie, L., Lei, T., and Ge, Z. (2019). Efficient enhancement of electron transport and collection capability in PTB7:$PC_{71}$BM-based solar cells enabled by sulforhodamine cathode interlayers. Chem. Asian J. *14*, 1472–1476.

Sun, K., Li, P., Xia, Y., Chang, J., and Ouyang, J. (2015). Transparent conductive oxide-free perovskite solar cells with PEDOT:PSS as transparent electrode. ACS Appl. Mater. Interfaces *7*, 15314–15320.

Vosgueritchian, M., Lipomi, D.J., and Bao, Z. (2012). Highly conductive and transparent PEDOT:PSS films with a fluorosurfactant for stretchable and flexible transparent electrodes. Adv. Funct. Mater. *22*, 421–428.

Wang, J., Fei, F., Luo, Q., Nie, S., Wu, N., Chen, X., Su, W., Li, Y., and Ma, C.Q. (2017). Modification of the highly conductive PEDOT:PSS layer for use in silver nanogrid electrodes for flexible inverted polymer solar cells. ACS Appl. Mater. Interfaces *9*, 7834–7842.

Wang, C., Sun, K., Fu, J., Chen, R., Li, M., Zang, Z., Liu, X., Li, B., Gong, H., and Ouyang, J. (2018). Enhancement of conductivity and thermoelectric property of PEDOT:PSS via acid doping and single post-treatment for flexible power generator. Adv. Sustain. Syst. *2*, 1800085.

Wen, Z., Yang, Y., Sun, N., Li, G., Liu, Y., Chen, C., Shi, J., Xie, L., Jiang, H., Bao, D., et al. (2018). A wrinkled PEDOT:PSS film based stretchable and transparent triboelectricnanogenerator for wearable energy harvesters and active motion sensors. Adv. Funct. Mater. *28*, 1803684.

Worfolk, B.J., Andrews, S.C., Park, S., Reinspach, J., Liu, N., Toney, M.F., Mannsfeld, S.C., and Bao, Z. (2015). Ultrahigh electrical conductivity in solution-sheared polymeric transparent films. Proc. Natl. Acad. Sci. U S A *112*, 14138–14143.

Xia, Y., Sun, K., and Ouyang, J. (2012). Solution-processed metallic conducting polymer films as transparent electrode of optoelectronic devices. Adv. Mater. *24*, 2436–2440.

Yan, C., Barlow, S., Wang, Z., Yan, H., Jen, A.K.Y., Marder, S.R., and Zhan, X. (2018). Non-fullerene acceptors for organic solar cells. Nat. Rev. Mater. *3*, 18003.

Yang, X., Hu, X., Wang, Q., Xiong, J., Yang, H., Meng, X., Tan, L., Chen, L., and Chen, Y. (2017). Large-scale stretchable semi-embedded copper nanowires transparent conductive films by electrospinning template. ACS Appl. Mater. Interfaces *9*, 26468–26475.

Yeon, C., Yun, S.J., Kim, J., and Lim, J.W. (2015). PEDOT:PSS films with greatly enhanced conductivity via nitric acid treatment at room temperature and their application as Pt/TCO-free counter electrodes in dye sensitized solar cells. Adv. Electron. Mater. *1*, 1500121.

Zhang, W., Zhao, B., He, Z., Zhao, X., Wang, H., Yang, S., Wu, H., and Cao, Y. (2013). High-efficiency ITO-free polymer solar cells using highly conductive PEDOT:PSS/surfactant bilayer transparent anodes. Energy Environ. Sci. *6*, 1956–1964.

Zhang, Y., Wu, Z., Li, P., Ono, L.K., Qi, Y., Zhou, J., Shen, H., Surya, C., and Zheng, Z. (2017). Fully solution-processed TCO-free semitransparent perovskite solar cells for tandem and flexible applications. Adv. Energy Mater. *8*, 1701569.

Zhang, S., Qin, Y., Zhu, J., and Hou, J. (2018). Over 14% efficiency in polymer solar cells enabled by a chlorinated polymer donor. Adv. Mater. *30*, 1800868.

Zhang, L., Yang, K., Chen, R., Zhou, Y., Chen, S., Zheng, Y., Li, M., Xu, C., Tang, X., Zang, Z., et al.

(2019). The role of mineral acid doping of PEDOT:PSS and its application in organic photovoltaics. Adv. Electron. Mater. https://doi.org/10.1002/aelm.201900648.

Zhao, G., Wang, W., Bae, T.S., Lee, S.G., Mun, C., Lee, S., Yu, H., Lee, G.H., Song, M., and Yun, J. (2015). Stable ultrathin partially oxidized copper film electrode for highly efficient flexible solar cells. Nat. Commun. *6*, 8830.

Zhao, G., Kim, S.M., Lee, S.-G., Bae, T.-S., Mun, C., Lee, S., Yu, H., Lee, G.-H., Lee, H.-S., Song, M., et al. (2016). Bendable solar cells from stable, flexible, and transparent conducting electrodes fabricated using a nitrogen-doped ultrathin copper film. Adv. Funct. Mater. *26*, 4180–4191.

Zhao, G., Song, M., Chung, H.S., Kim, S.M., Lee, S.G., Bae, J.S., Bae, T.S., Kim, D., Lee, G.H., Han, S.Z., et al. (2017). Optical transmittance enhancement of flexible copper film electrodes with a wetting layer for organic solar cells. ACS Appl. Mater. Interfaces *9*, 38695–38705.

Zhou, L., Yu, M., Chen, X., Nie, S., Lai, W.-Y., Su, W., Cui, Z., and Huang, W. (2018). Screen-printed poly(3,4-ethylenedioxythiophene): poly(styrenesulfonate) grids as ITO-free anodes for flexible organic light-Emitting diodes. Adv. Funct. Mater. *28*, 1705955.

**iScience, Volume *23***

## Supplemental Information

# Over 14% Efficiency Folding-Flexible ITO-free Organic Solar Cells Enabled by Eco-friendly Acid-Processed Electrodes

**Wei Song, Ruixiang Peng, Like Huang, Chang Liu, Billy Fanady, Tao Lei, Ling Hong, Jinfeng Ge, Antonio Facchetti, and Ziyi Ge**

# Supplemental Information

## Over 14% Efficiency Folding-flexible ITO-free Organic Solar Cells Enabled by Eco-friendly Acid-Processed Electrodes

Wei Song[1,2], Ruixiang Peng[1,2], Like Huang[1], Chang Liu[1], Billy Fanady[1] Tao Lei[1,2], Ling Hong[1,2], Jinfeng Ge[1], Antonio Facchetti[3], Ziyi Ge[1,2,4,*]

[1] Ningbo Institute of Materials Technology and Engineering, Chinese Academy of Sciences, Ningbo, 315201, China

[2] Center of Materials Science and Optoelectronics Engineering, University of Chinese Academy of Sciences, Beijing 100049, China

[3] Department of Chemistry, Northwestern University, 2145 Sheridan Road, Evanston, Illinois 60208, United States

[4] Lead Contact

Correspondence: *E-mail: geziyi@nimte.ac.cn

## Transport Method

***Materials:*** PBDB-T-2F, Y6 and PDINO were purchased from Solarmer Materials Inc, Beijing, the molecular weight and dispersity of PM6 are Mn: 36kDa and PDI: 2.5-2.7, respectively. Citric acid, tartaric acid and malic acid were purchased from Acros Inc. The indium-doped tin oxide (ITO)-coated polyethylene terephthalate (PET) (≤15 Ω/square) was purchased from South China Xiangcheng Technology Co., Ltd. Two types of PEDOT:PSS, or Poly(3,4-ethylenedioxythiophene):poly(styrenesulfonate), aqueous solutions (i.e., Clevios PH1000 with a solid content of 1.0-1.3% and Clevios P VP 4083) were purchased from Heraeus, Germany.

***Preparation of PEDOT:PSS FTEs*:** PET (~140 μm) and glass substrates with an area of 1.5×1.5 $cm^2$ were sequentially cleaned by ultrasonic treatment in deionized (DI) water, acetone and isopropanol (IPA). The pristine PEDOT:PSS and m-PEDOT:PSS (doped with 0.5% D-sorbitol) electrodes were prepared by spin coating of a PEDOT:PSS aqueous solution (Clevios PH1000, Heraeus, Germany) doped with 0.3 vol% Zonyl FS300 at 2,000 rpm. These PEDOT:PSS solutions were filtered through a 0.45 μm syringe filter before applying it on a PET substrate for spin coating. Next, the PEDOT:PSS films were dried at 90°C on a hot plate for 15 min. The optimum concentration of the eco-friendly acid solution (such as citric acid, malic acid and tartaric acid) was dropwise applied on the surface of PEDOT:PSS film and retained for 15 min, then the acid-treated films were washed with DI water, ethanol and glycol for 3 times each to remove residual acid. Finally, it was dried on a heating table at 90° C for 15 min to form a highly conductive PEDOT:PSS electrodes.

***OSC fabrication*:** OSC devices based on PEDOT:PSS and ITO electrodes were fabricated. The ITO electrode was treated by UV-ozone to enhance surface wettability prior to deposition of the PEDOT:PSS buffer layer. The PEDOT:PSS (Clevios P VP 4083) solution was spin coated on a PEDOT:PSS FTE (60 nm) or ITO electrode at 2,500 rpm and then dried at 90°C for 20 min to form an anode buffer layer (35 nm). Then, the active layer (100 nm) was deposited by spin coating a chloroform solution consisting of PBDB-T-2F:Y6 (1:1.2 w/w, 16 mg/mL in total) with 0.7 vol% of 1-chloronaphthalene (CN) additives at 2,500 rpm for 1 min, followed by a thermal annealing at 90 °C for 10 min in a $N_2$-filled glove box. Subsequently, PDINO dissolved in methanol (1.5 mg/mL) were spin-coated on the active layers at 3,000 rpm to act as the cathode buffer layer. Finally, Al electrodes (thickness: ~100 nm) were thermally evaporated under a shadow mask at $10^{-4}$ Pa. The shadow mask has 8 square holes with a dimension of 2.0×2.0 mm, ensuing a precise active area of 4.0 $mm^2$.

***Characterizations*:** Electrical contacts were made by Ag paste and indium materials on the four corners of each PEDOT:PSS film. The square resistances of samples were measured using the 4-Point Probes Measurement System (CRESBOX). Film thickness was measured by a surface profile-meter (Dektak 150). The adhesion force of PEDOT:PSS solution was measured by a high sensitivity micro electro mechanical balance system (Data-Physics DCAT21, Germany). The UV-transmission spectra of the polymer films were taken with a Hitachi U-3010 UV−vis spectrophotometer, and the AFM images of the polymer films were obtained using atomic force microscope (VEECO Dimension 3100V). The EDS images of the polymer films were obtained using transmission electron microscope (Verios G4 UC). Compositions and chemical states of films were examined by XPS (XSAM800). Using a Keithley 2440 source-measure unit integrated with AM 1.5G solar simulator (Newport-Oriel Sol3A 450 W), *J–V* characteristics of the solar cells were carried out in $N_2$-filled glove box. The light intensity was calibrated with a standard silicon detector. To evaluate the flexibility of the flexible devices, the devices were placed on a cylindrical surface with a radius of 4 mm or by folding the device. It then underwent a specific number of repeated bending before re-measurement of the device to test for the change in performance.

## Optical and Electrical Characteristics of PEDOT:PSS

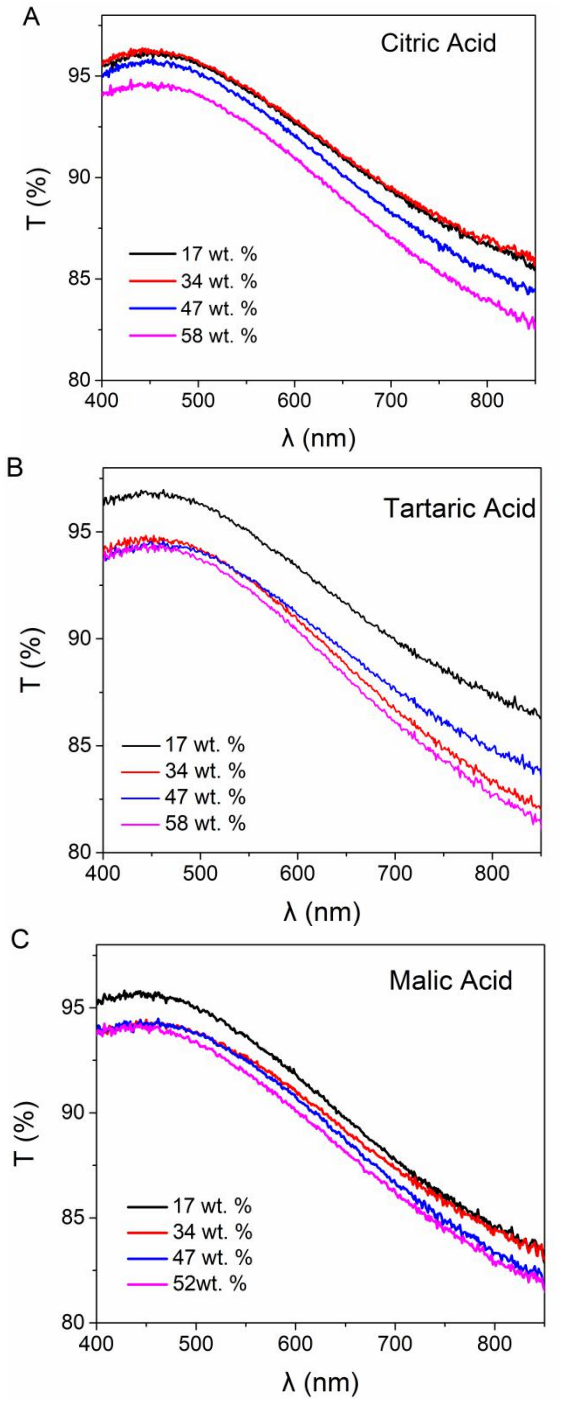


**Figure S1.** Optical transparency of the PEDOT:PSS films with three kinds of acid treatments at different concentrations

**Figure S1** shows the optical transparency (*T*) spectra of the PEDOT:PSS films with three kinds of eco-friendly acid treatments at different concentrations. The saturation of citric acid, tartaric acid and malic acid in deionized water are approximately 58 wt.%, 58 wt.% and 52 wt.%, respectively. It can be shown that the PEDOT:PSS films with the three green acids treatments exhibited a broad plateau above 85.0% in the visible and near-infrared regions, making it to be a good choice for transparent conductive electrodes for organic solar cells. The highly transparent conductive films are resulted from a removal of hydrophilic PSS from PEDOT:PSS matrix and a better stack of PEDOTs induced by the eco-friendly acid treatments at different concentrations.

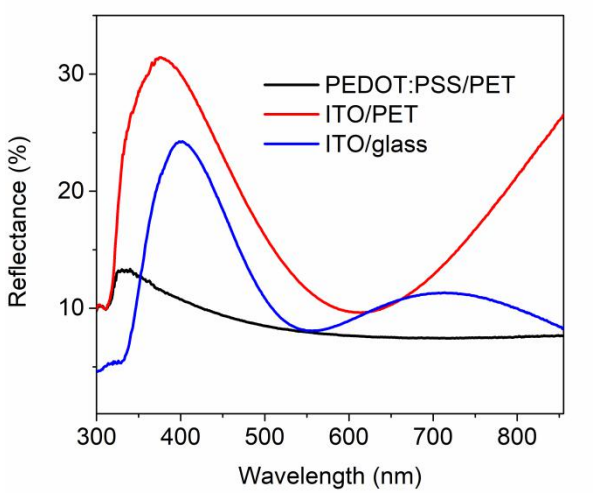


**Figure S2.** Reflectance spectra of ITO/glass, ITO/PET and citric acid-treated PEDOT:PSS/PET.

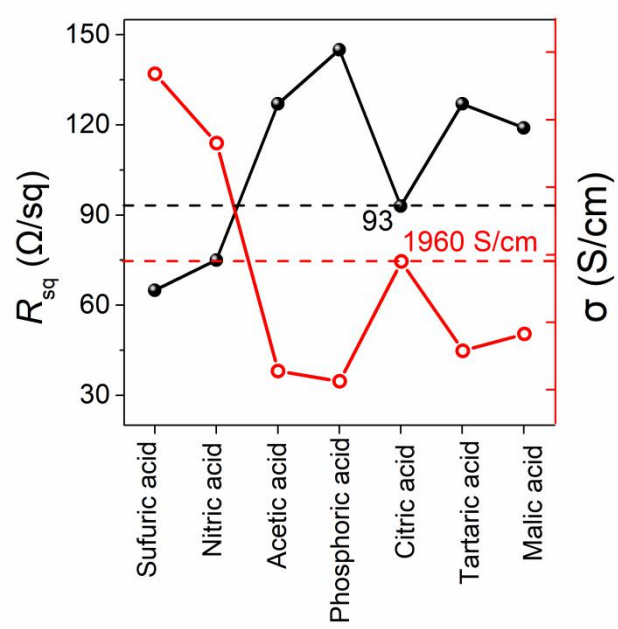


**Figure S3.** Comparison of square resistance and electrical conductivity of PEDOT:PSS films with various acid treatment.

**Energy banding analysis (UPS)**

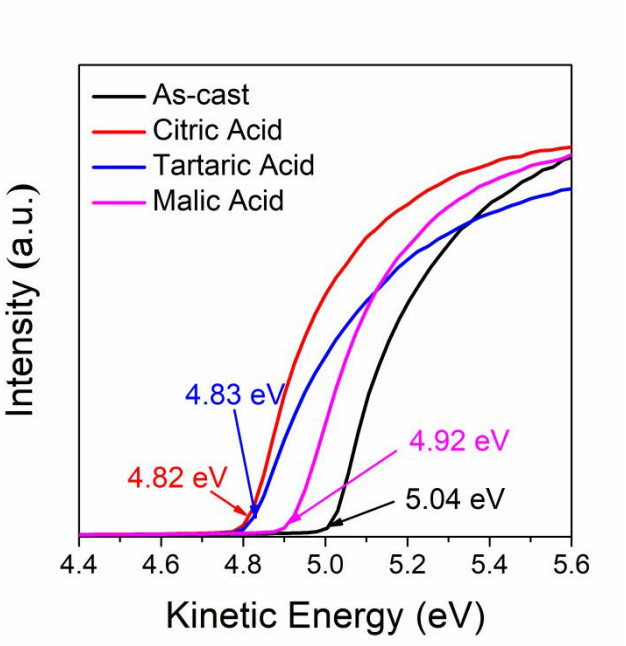


**Figure S4.** Ultraviolet photoelectron spectroscopy (UPS) of pristine PEDOT:PSS film, and PEDOT:PSS films with citric acid, tartaric acid and malic acid treatment, respectively.

## Morphology Analysis of PEDOT:PSS

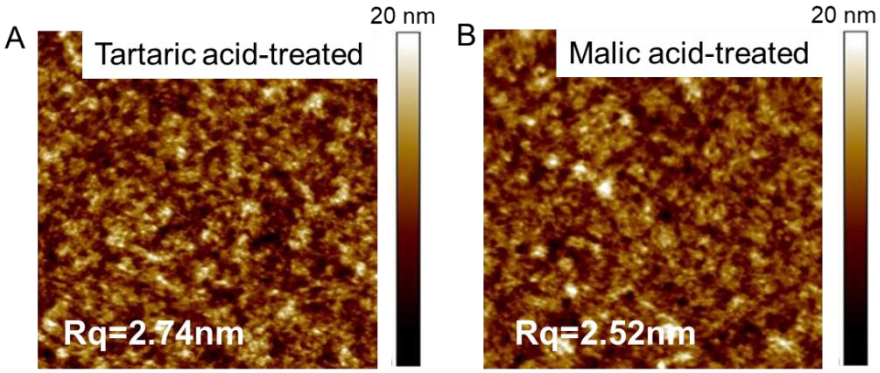


**Figure S5.** AFM images of the A) tartaric acid-treated, B) malic acid-treated PEDOT:PSS films on PET plastic substrates. Scale bar: 2 × 2 $\mu m^2$.

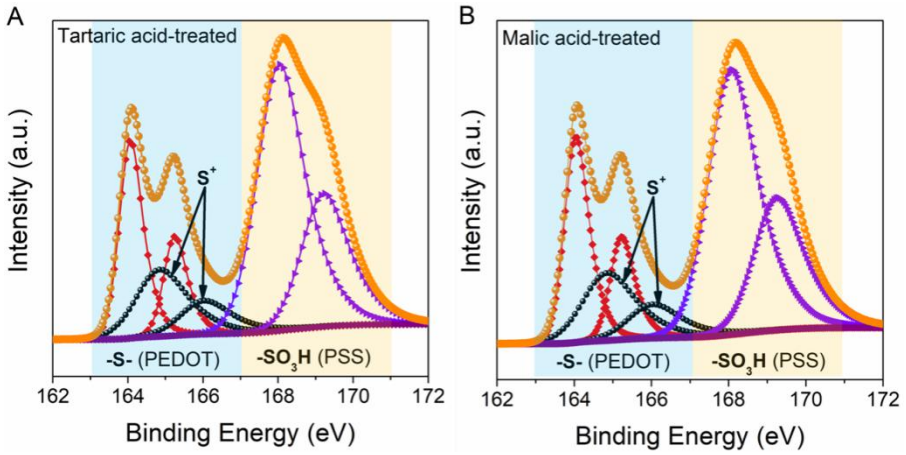


**Figure S6.** Fitted S 2p XPS spectra A) the films with optimal concentration tartaric acid treatments, and B) the films with optimal concentration malic acid treatments.

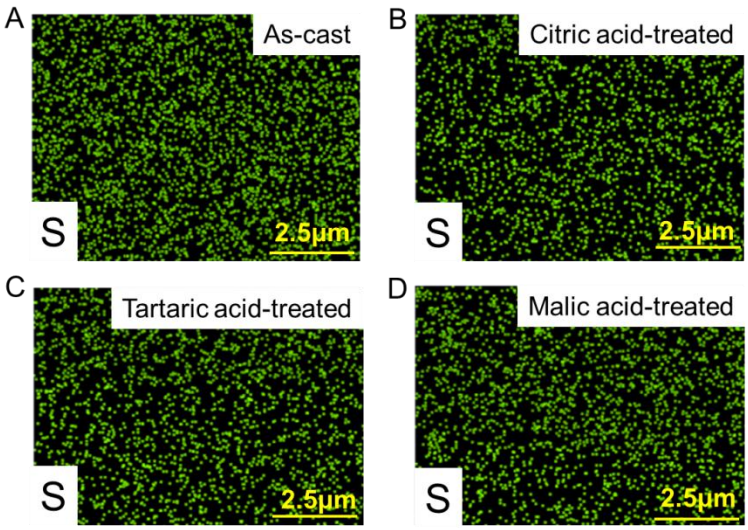


**Figure S7.** EDS elemental mapping showing the distribution of the S element in A) as-cast, B) citric acid-treated, C) tartaric acid-treated, D) malic acid-treated PEDOT:PSS films.

**Figure S5** shows the atomic force microscopy (AFM) images of the films with different eco-friendly acid treatments. The PEDOT:PSS film with tartaric acid and malic acid treatments exhibited a larger phase separation as it showed a RMS as high as 2.74 nm, and 2.52 nm. When highly concentrated green acid is dropped on the as-cast PEDOT:PSS film, $H^+$ from the eco-friendly acids will associate with the $PSS^-$ to form neutral PSSH in the PEDOT:PSS films.

Explosion atom contents and element states of PEDOT:PSS effective method applicable X-ray photoelectron spectroscopy (XPS). **Figure S6** shows the S 2p X-ray photoelectron spectroscopy (XPS) of the films with tartaric acid and malic acid treatments. Notably, the XPS bands between 167 and 171 eV are mainly originated from the sulfonate moieties ($–SO_3H$) of PSS, whereas, the XPS bands between 163 and 167 eV are mainly originated from thiophene rings (–S–) of PEDOT. For the as-cast and acid-treated PEDOT:PSS film, the fitted peaks colored in black correspond to the $S^+$. Our curve fitting results showed that the PSSH peak intensity was significantly reduced for the three acid-treated samples to contributes to the high FoM, indicating that some PSSH was significantly removed after the green acid treatments of PEDOT:PSS. It was found that removal of a large amount of PSS components from the PEDOT:PSS matrix resulted in structural rearrangement of PEDOT with enhanced crystallinity.

**Figure S7** shows EDS elemental mapping distribution of the S element in the films with as-cast, citric acid, tartaric acid and malic acid treatments, respectively. EDS elemental mapping shows that the distribution of S elements in the film after eco-friendly acid treatments is rare compared with the S element of pristine PEDOT:PSS film distribution.

## Molecular structures and energy levels alignment

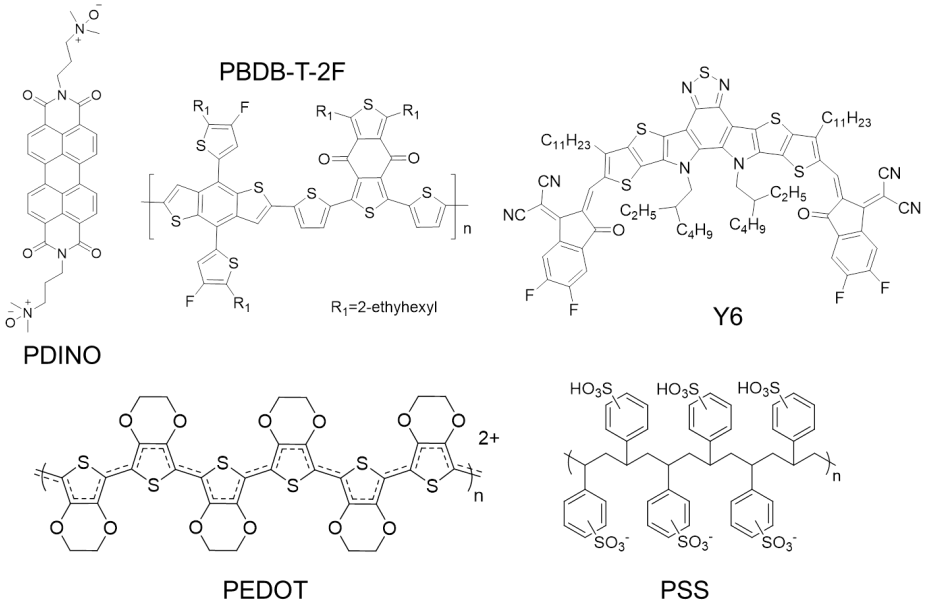


**Figure S8.** Molecular structures of PBDB-T-2F, Y6, PDINO and PEDOT:PSS, respectively.

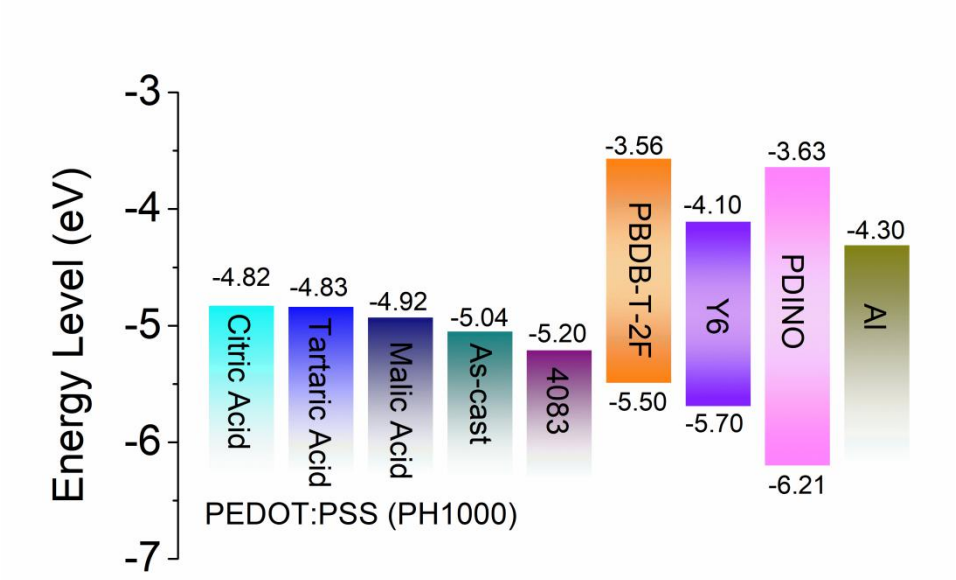


**Figure S9.** Energy levels alignment of the layers of flexible devices.

## External quantum efficiency spectra

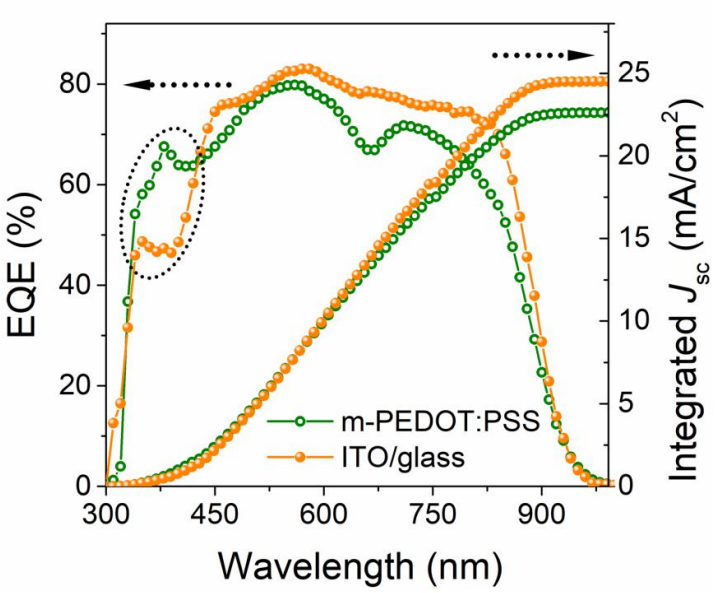


**Figure S10.** EQE spectra of the PSCs based on PM6:Y6 (1:1.2, w/w) with citric acid-treated m-PEDOT:PSS/PET as flexible transparent electrode and ITO/glass transparent electrode.

**Table S1.** Conductivities and square resistances of various acid-treated PEDOT:PSS films.

| Post-treatment | Characteristics | Chemical formula | $pK_a$ | $R_{sq}$ ($\Omega$ $sq^{-1}$) | $\sigma$ (S $cm^{-1}$) | $d_f$ ( nm) | FoM |
|---|---|---|---|---|---|---|---|
| **Sulfuric acid**[a] [98 wt. %] | Strong corrosion | $H_2SO_4$ | -3.0 | 65 | 3070 | 50 | 60 |
| **Nitric acid**[b] [68 wt. %] | Strong corrosion | $HNO_3$ | -2.0 | 75 | 2660 | 50 | 32 |
| **Phosphoric acid** [85 wt. %] | Strong corrosion | $H_3PO_4$ | 2.2, 7.2, 12.3 | 145 | 1250 | 55 | 33 |
| **acetic acid** [99 wt. %] | Strongly volatile | $C_2H_4O_2$ | 4.8 | 127 | 1310 | 60 | 32 |
| **Citric acid** [58 wt. %] | eco-friendly | $C_6H_8O_7$ | 3.1, 4.8, 6.4 | 93 | 1960 | 55 | 54 |
| **Tartaric acid** [58 wt. %] | eco-friendly | $C_4H_6O_6$ | 3.0, 4.3 | 119 | 1530 | 55 | 39 |
| **Malic acid** [52 wt. %] | eco-friendly | $C_4H_6O_5$ | 3.5, 5.1 | 127 | 1430 | 55 | 34 |

**Table S2.** Comparison of PCE values of flexible organic solar cells with diverse flexible transparent electrodes.

| FTE categories | Post-treatment | Active layer | Ave. PCE (%) | Refer. |
|---|---|---|---|---|
| **PEDOT:PSS** | | | | |
| PEDOT:PSS | sulfuric acid | PTB7-Th:$PC_{71}BM$ | 7.7 | Kim et al., 2015 |
| PEDOT:PSS | methanesulfonic acid | PBDTT-S-TT:$PC_{71}BM$ | 6.42 | Fan et al., 2016 |
| PEDOT:PSS | methanesulfonic acid | PBDB-T-2Cl:IT-4F | 12.35 | Peng et al., 2019 |
| PEDOT:PSS | methanol | P3HT:PCBM | 2.87 | Worfolk et al., 2015 |
| PEDOT:PSS | phosphoric acid | P3HT:ICBA | 3.33 | Meng et al., 2015 |
| PEDOT:PSS | | P3HT:PCBM | 4.2 | Kaltenbrunner et al., 2012 |
| PEDOT:PSS | citric acid | PBDB-T-2F:Y6 | 13.94 | **Our work** |
| m-PEDOT:PSS | citric acid | | 14.17 | |
| PEDOT:PSS | tartaric acid | | 13.47 | |
| PEDOT:PSS | malic acid | | 12.90 | |
| **PEDOT:PSS/Metal** | | | | |
| PEDOT:PSS/Ag island | | PTB7-Th:$PC_{71}BM$ | 9.8 | Kang et al., 2015 |
| PEDOT:PSS/Ag grid | | PTB7-Th:$PC_{71}BM$ | 6.58 | Wang et al., 2017 |
| PEDOT:PSS/Ag mesh | | PTB7:$PC_{71}BM$ | 6.73 | Kim et al., 2016 |
| PEDOT"PSS/Ag Nanowire | | PM6:IT-4F | 10.30 | Lei et al., 2019 |
| PEDOT:PSS/ITO | | PBDB-T-2F:Y6 | 13.5 | Lei et al., 2019 |
| **ZnO/metal/ZnO** | | | | |
| ZnO/Cu(8.0 nm) on Cu(O)/ZnO | | PTB7:$PC_{71}BM$ | 6.70 | Zhao et al., 2016 |
| ZnO/Cu(9.5 nm) on Cu(O)/ZnO | | PTB7:$PC_{71}BM$ | 7.7 | Zhao et al., 2017 |
| $TiO_2$/ZnO/Ag(8.0 nm)/ZnO | | PBDB-T:IT-M:$PC_{71}BM$ | 10.48 | Liu et al., 2017 |
| ZnO/Cu (O:5%)(7 nm)/ZnO | | PTB7-Th:$PC_{71}BM$ | 7.65 | Zhao et al., 2015 |
| ZnO/N-doped Cu(6.5 nm)/ZnO | | PTB7:$PC_{71}BM$ | 7.10 | Zhao et al., 2016 |
| **Metal nano-structures** | | | | |
| Ag grid | | PTB7-Th:$PC_{71}BM$ | 6.43 | Lu et al., 2017 |
| Ag NW | | PTB7-Th:$PC_{71}BM$ | 8.75 | Seo et al., 2017 |
| Cu NW | | PTB7-Th:$PC_{71}BM$ | 4.6 | Yang et al., 2017 |
| **Others** | | | | |
| Graphene | | PTB7:$PC_{71}BM$ | 7.2 | Park et al., 2014 |
| CNT | | PTB7:$PC_{71}BM$ | 3.91 | Jeon et al., 2015 |
| ITO | | PCE-10:IEICO-4F | 12.5 | Xiong et al., 2019 |

## Supplemental References


Kim, N., Kang, H., Lee, J. H., Kee, S., Lee, S. H., Lee, K. (2015). Highly conductive all-plastic electrodes fabricated using a novel chemically controlled transfer-printing method. Adv. Mater. *27*, 2317–2323.

Fan, X., Xu, B., Liu, S., Cui, C., Wang, J., Yan, F. (2016). Transfer-printed PEDOT:PSS electrodes using mild acids for high conductivity and improved stability with application to flexible organic solar cells. ACS Appl. Mater. Inter. *8*, 14029-14036.

Peng, R., Song, W., Yan, T., Fanady, B., Li, Y., Zhan, Q., Ge, Z. (2019). Interface bonding engineering of a transparent conductive electrode towards highly efficient and mechanically flexible ITO-free organic solar cells. J. Mater. Chem. A *7*, 11460-11467.

Worfolk, B. J., Andrews, S. C., Park, S., Reinspach, J., Liu, N., Toney, M. F., Mannsfeld, S. C., Bao, Z. (2015). Ultrahigh electrical conductivity in solution-sheared polymeric transparent films. Natl Acad. Sci. USA *112*, 14138-14143.

Meng, W., Ge, R., Li, Z., Tong, J., Liu, T., Zhao, Q., Xiong, S., Jiang, F., Mao, L., Zhou, Y. (2015). Conductivity enhancement of PEDOT:PSS films via phosphoric acid treatment for flexible all-plastic solar cells. ACS Appl. Mater. Inter. *7*, 14089-14094.

Kaltenbrunner, M., White, M. S., Glowacki, E. D., Sekitani, T., Someya, T., Sariciftci, N. S., Bauer, S. (2012). Ultrathin and lightweight organic solar cells with high flexibility. Nat. Commun. *3*, 770.

Kang, H., Jung, S., Jeong, S., Kim, G., Lee, K. (2015). Polymer-metal hybrid transparent electrodes for flexible electronics. Nat. Commun. *6*, 6503.

Wang, J., Fei, F., Luo, Q., Nie, S., Wu, N., Chen, X., Su, W., Li, Y., Ma, C. Q. (2017). Modification of the highly conductive PEDOT:PSS layer for use in silver nanogrid electrodes for flexible inverted polymer solar cells. ACS Appl. Mater. Inter. *9*, 7834-7842.

Kim, W., Kim, S., Kang, I., Jung, M. S., Kim, S. J., Kim, J. K., Cho, S. M., Kim, J.-H., Park, J. H. (2016). Hybrid silver mesh electrode for ITO‐free flexible polymer solar Cells with good mechanical stability. ChemSusChem *9*, 1042-1049.

Lei, T., Peng, R., Song, W., Hong, L., Huang, J., Fei, N., Ge, Z. (2019). Bendable and foldable flexible organic solar cells based on Ag nanowire films with 10.30% efficiency. J. Mate. Chem. A *7*, 3737-3744.

Lei, T., Peng, R., Huang, L., Song, W., Yan, T., Zhu, L., Ge, Z. (2019). 13.5% flexible organic solar cells achieved by robust composite ITO/ PEDOT:PSS electrodes. Mater. Today Energy *14*. 100334.

Zhao, G., Kim, S. M., Lee, S. G., Bae, T. S., Mun, C. W., Lee, S., Yu, H., Lee, G. H., Lee, H. S., Song, M., et al. (2016). Bendable solar cells from stable, flexible, and transparent conducting electrodes fabricated using a nitrogen‐doped ultrathin copper film. Adv. Funct. Mater. *26*, 4180.

Zhao, G., Song, M., Chung, H. S., Kim, S. M., Lee, S. G., Bae, J. S., Bae, T. S., Kim, D., Lee, G. H., Han, S. Z., et al. (2017). Optical transmittance enhancement of flexible copper film electrodes with a wetting layer for organic solar cells. ACS Appl. Mater. Inter. *9*, 38695-38705.

Liu, Q., Toudert, J., Ciammaruchi, L., Martínez-Denegri, G., Martorell, J. (2017). High open-circuit voltage and short-circuit current flexible polymer solar cells using ternary blends and ultrathin Ag-based transparent electrodes. J. Mater. Chem. A *5*, 25476-25484.

Zhao, G., Wang, W., Bae, T. S., Lee, S. G., Mun, C., Lee, S., Yu, H., Lee, G. H., Song, M., Yun, J. (2015). Stable ultrathin partially oxidized copper film electrode for highly efficient flexible solar cells. Nat. Commun. *6*, 8830.

Zhao, G., Kim, S. M., Lee, S.-G., Bae, T.-S., Mun, C., Lee, S., Yu, H., Lee, G.-H., Lee, H.-S., Song, M., et al. (2016). Bendable solar cells from stable, flexible, and transparent conducting electrodes fabricated using a

nitrogen‐doped ultrathin copper film. Adv. Funct. Mater. *26*, 4180-4191.

Lu, S., Lin, J., Liu, K., Yue, S., Ren, K., Tan, F., Wang, Z., Jin, P., Qu, S., Wang, Z. (2017). Large area flexible polymer solar cells with high efficiency enabled by imprinted Ag grid and modified buffer layer. Acta Mater. *130*, 208-214.

Seo, J. H., Hwang, I., Um, H. D., Lee, S., Lee, K., Park, J., Shin, H., Kwon, T. H., Kang, S. J., Seo, K. (2017). Cold isostatic‐pressured silver nanowire electrodes for flexible organic solar cells via room‐temperature processes. Adv. Mater. *29*, 1701479.

Yang, X., Hu, X., Wang, Q., Xiong, J., Yang, H., Meng, X., Tan, L., Chen, L., Chen, Y. (2017). Large-scale stretchable semiembedded copper nanowire transparent conductive films by an electrospinning template. ACS Appl. Mater. Inter. *9*, 26468-26475.

Park, H., Chang, S., Zhou, X., Kong, J., Palacios, T., Gradecak, S. (2014). Flexible Graphene Electrode-Based Organic Photovoltaics with Record-High Efficiency. Nano lett. *14*, 5148-5154.

Jeon, I., Cui, K., Chiba, T., Anisimov, A., Nasibulin, A. G., Kauppinen, E. I., Maruyama, S., Matsuo, Y. (2015). Direct and dry deposited single-walled carbon nanotube films doped with $MoO_x$ as electron-blocking transparent electrodes for flexible organic solar cells. J. Am. Chem. Soc. *137*, 7982-7985.

Xiong, S., Hu, L., Hu, L., Sun, L., Qin, F., Liu, X., Fahlman, M., Zhou, Y. (2019). 12.5% flexible nonfullerene solar cells by passivating the chemical interaction between the active layer and polymer interfacial layer. Adv. Mater. *31*, e1806616.